International Journal of Medical Microbiology 309 (2019) 151330

Contents lists available at ScienceDirect

International Journal of Medical Microbiology

journal homepage: www.elsevier.com/locate/ijmm

ADH1 promotes *Candida albicans* pathogenicity by stimulating oxidative phosphorylation

Yanjun Song[a,b,1], Shuixiu Li[a,b,1], Yajing Zhao[a,b,1], Yishan Zhang[a,b,1], Yan Lv[a,b], Yuanying Jiang[c], Yan Wang[c], Dongmei Li[d], Hong Zhang[a,b,*]

[a] The First Affiliated Hospital of Jinan University, Guangzhou, Guangdong, China
[b] Institute of Mycology, Jinan University, Guangzhou, Guangdong, China
[c] New Drug Research and Development Center, School of Pharmacy, Second Military Medical University, Shanghai, China
[d] Department of Microbiology and Immunology, Georgetown University Medical Center, Washington, DC, USA

ARTICLE INFO

Keywords:
ADH1
Candida albicans
Pathogenicity
Oxidative phosphorylation

ABSTRACT

Objective: Alcohol dehydrogenase I is encoded by *ADH1* in *Candida albicans*, and is one of the key enzymes in fungal metabolism by which it catalyzes the conversion from acetaldehyde to ethanol. The role of the associated protein Adh1p, encoded by *ADH1* in fungal pathogenicity has not been thoroughly studied despite its near ubiquity in the fungal kingdom. Using *C. albicans* as a model, this study proposes to determine the possible pathogenic roles for *ADH1* and its possible underlying mechanisms.

Methods: The *SAT1* flipper strategy was used to construct the *ADH1* deletion mutant. Growth curves and spot assay were used to compare growth and cell viability of the mutant to wild type *C. albicans*. Three host model systems (infected mice, *C. elegans*, and *G. mellonella*) were used to investigate the effects of *ADH1* deletion *in vivo* on *C. albicans* pathogenicity. Then, adhesion, hyphal formation, biofilm formation, cell surface hydrophobicity (CSH) and RT-qPCR were performed to investigate the effects of *ADH1* deletion *in vitro* on *C. albicans* virulence. Finally, Xfe 96 seahorse assay, ROS level, mitochondrial membrane potential, and intracellular ATP content were used to determine the effects of *ADH1* deletion on bioenergetics.

Results: *ADH1* deletion has no effects on the growth and cell viability of *C. albicans*, but significantly prolongs survival time in each of the three host models, decreases fungal burden in kidney and liver, and lessens pathological tissue damage ($P < 0.05$). In addition, *ADH1* deletion significantly increases CSH and reduces *C. albicans* virulence in terms of adhesion, hyphal formation and biofilm formation in accord with the down-regulation of virulence-related genes such as *ALS1, ALS3, HWP1*, and *CSH1* ($P < 0.05$). For bioenergetics, *ADH1* deletion has no obvious effect on glycolysis, but a lack of *ADH1* significantly increases ROS levels and decreases mitochondrial membrane potential and intracellular ATP content even through the mitochondrial oxygen consumption rate and $NADH/NAD^+$ ratio are elevated ($P < 0.05$).

Conclusion: Our results suggest that the fermentative enzyme *ADH1* is required for the pathogenicity of *C. albicans* under one of the presumed mechanisms *via*its effects on oxidative phosphorylation activities in mitochondria.

1. Introduction

Alcohol dehydrogenases in the model yeast *Saccharomyces cerevisiae* catalyse a reversible dehydrogenation and hydrogenation between ethanol and acetaldehyde metabolism which is known to be important for energy production and storages. Adh1p, encoded by *ADH1* in *Candida albicans*, carries out the major role in alcohol oxidation. Deletion of *ADH1* increased acetaldehyde production and decreased alcohol production (Mukherjee et al., 2006; Chen et al., 2014; Zhang et al., 2018a, 2018b). Also, the mutant strain exhibited a high intracellular methylglyoxal concentration (Kwak et al., 2014), which is required for NADH oxidation and alcohol production from the breakdown of amino acids *via*the Ehrlich pathway (Hazelwood et al., 2008).

The alcohol dehydrogenase protein family forms the key components of the fungal fermentation process. When pyruvate produced from glycolysis is converted to acetaldehyde and carbon dioxide, the

* Correspondence author at: Institute of Mycology, Jinan University, 601 Huangpu Avenue West, Guangzhou, Guangdong, 510632, China.
E-mail address: tzhangh@jnu.edu.cn (H. Zhang).
[1] These authors contributed equally to this work.

https://doi.org/10.1016/j.ijmm.2019.151330
Received 18 January 2019; Received in revised form 24 June 2019; Accepted 9 July 2019

acetaldehyde is then reduced to ethanol by alcohol dehydrogenase I (Adh1p). As the reduction step is also used by yeast cells to regenerate NAD^+, this alcohol and acetaldehyde conversion is the prerequisite condition for continuity of the energy-generating glycolysis (Leskovac et al., 2002).

The association of Adh1p with microbial pathogenicity have been noticed in some microorganism models, however, systemic studies are still lacking, and to date, similar studies to address Adh1p in *C. albicans* virulence are still fragmentary. For example, *ADH1* was shown to up-regulate biofilm formation by *Staphylococcus aureus* (Becker et al., 2001); *ADH1* deletion resulted in decreased *Fusarium oxysporum* virulence (Corrales Escobosa et al., 2011); Kwak et al. (Kwak et al., 2014) reported that *ADH1* deletion attenuated hyphal formation and virulence (likely by increasing the intracellular methylglyoxal concentration); and finally, Mukherjee et al. (Mukherjee et al., 2006) reported that *ADH1* deletion enhanced biofilm formation due to decreased ethanol. Others have reported that Adh1p has other multiple roles in *C. albicans* pathogenesis, including interactions with the host immune system (Pitarch et al., 2004) and binding host proteins (Klotz et al., 2001). Adh1p is the *C. albicans* cell wall protein able to bind plasminogen, which leads to the release of activated plasmin with the function of proteolytic activity (Crowe et al., 2003), suggesting it may promote *C. albicans* invasion of host tissues. Adh1p is immunogenic in humans and acts as a fibronectin receptor to participate in the pathogenesis process (Bertram et al., 1996). Which then begs the question, what is the role of *ADH1* in the pathogenicity of *C. albicans*?

In this study, we first construct the *ADH1* deletion mutant and revertant strain by *SAT1* flipper strategy using *C. albicans* wild-type strain as SC5314 the parental strain. By comparing with wild type at each step, we systematically evaluate the roles of the *ADH1* in the pathogenicity of *C. albicans in vivo* and *in vitro*, and propose the likely underlying mechanisms. We confirm that *ADH1* deletion significantly attenuates the virulence of *C. albicans* in the three host model systems and significantly reduces the virulence factors of *C. albicans in vitro*. The mechanism study *in vitro* suggests that *ADH1* deletion may attenuate pathogenicity of *C. albicans* by changing the metabolic status of the organism by decreasing intracellular ATP content.

2. Materials and methods

2.1. Construction of ADH1 deletion and reconstituted strains and growth conditions

The strains used in this study are listed in Supplementary Table S1. In brief, the *SAT1* flipper strategy was used to delete both alleles of *ADH1* in *C. albicans* SC5314 (Fig. S1). One copy of the *ADH1* gene was returned to the *ADH1* locus to form the constituted strain (Fig. S2). A null mutant of *ADH1* (*adh1*Δ/Δ) was constructed by PCR-mediated homologous recombination as described previously (Sasse and Morschhäuser, 2012). *C. albicans* wild type strain SC5314 (Gillum et al., 1984) was used to generate the *adh1*Δ/Δ mutant strain (*adh1*Δ::FRT/*adh1*Δ::FRT) and *adh1*Δ/*ADH1* reconstituted strain (*adh1*Δ::FRT/*ADH1*::FRT). The primers used for gene deletion in this study were listed in Supplementary Table S2. The confirmation of the*adh1*Δ/Δ mutant and reconstituted strain (*adh1*Δ/*ADH1*) were performed by PCR amplicons using primer pairs as shown in Supplementary Fig. S1-S5.

All the strains were routinely grown in YPD broth or on YPD agar (1% yeast extract, 2% peptone, 2% glucose and 2% agar) unless explicitly indicated otherwise.

2.2. Experimental animals

Sixty specific pathogen-free female ICR mice (6–8 weeks old, 18–22 g) were purchased from Shanghai Slack Laboratory Animals Co., Ltd. (animal certification number: SCXK, Shanghai 2007-0005). All animal experiments were conducted in the animal laboratory facility of the School of Pharmacy of Second Military Medical University. *Escherichia coli* OP50 and *Caenorhabditis elegans* (*glp-4;sek-1* gene-deficient) were kindly provided as a gift by Professor Eleftherios Mylonakis from Harvard University (USA) (Pukkila-Worley et al., 2009).

2.3. Growth kinetics

Strains were separately cultured in yeast extract-peptone-dextrose (YPD) liquid medium. Cells in the late exponential growth phase were harvested by centrifugation, washed twice with sterile phosphate-buffered saline (PBS), and then resuspended in YPD liquid medium. The concentration of the yeast suspension was adjusted to optical density at 600 nm (OD_{600}) = 0.04. The obtained suspension was placed in a 250-mL Erlenmeyer flask and cultured at 30 °C with shaking at 200 rpm. The OD_{600} value of each yeast suspension was measured at 0, 2, 4, 6, 8, 10, 12 and 24 h to plot the growth curve of the strain. The doubling time (DT) at the logarithmic growth phase was calculated based on the concentration of the yeast suspension: $DT = t \times lg2/lg[N_t/N_0]$ (where N_t is the number of yeast cells at time t, and N_0 is the initial yeast cell count) (Reuss et al., 2004).

A spot assay was performed to investigate the effect of the *ADH1* deletion on the cell viability of *C. albicans* (Noble and Johnson, 2007)· *C. albicans* strains were cultured in YPD liquid medium at 30 °C with shaking at 200 rpm overnight. The cells were collected by centrifugation, washed twice with sterile PBS, and resuspended; the concentration of yeast cells was adjusted to 1.0×10^6 cells/mL. The yeast suspension was 10-fold serially diluted in sterile PBS to prepare five stock suspensions. A total of 5 μL of each stock suspension was plated on the surface of YPD, YPG (1% yeast extract, 2% peptone, 2% glycerol and 2% agar), YPE (1% yeast extract, 2% peptone, 2% ethanol and 2% agar), YPO (1% yeast extract, 2% peptone, 2% oleic acid and 2% agar) and YPC (1% yeast extract, 2% peptone, 2% citrate and 2% agar) solid medium. The plates were cultured at 30℃ for 48 h before observing the growth of colonies.

2.4. Effect of ADH1 deletion on C. albicans virulence in mice

A mouse model of disseminated candidiasis was used to evaluate the virulence of the strains (Spellberg et al., 2003, 2005). Female ICR mice were used for all experiments. Mice were injected *via*the lateral tail vein with a suspension of 1.0×10^5 cells from each strain. Survival rate was calculated from 10 infected mice per strain. For determination of fungal burden, another three mice from each group were euthanized after 48 h infection. Kidney was harvested, weighed, homogenized, and quantitatively cultured. In addition, at day 1 of infection, mice were killed and organs removed to fix in 4% buffered formalin, then embed in paraffin, sectioned and stained with Periodic Acid-Schiff for histological study. Mortality was represented with Kaplan-Meier survival curves and quantitative tissue burdens were marked in the log scale and compared in the Mann-Whitney test.

2.5. C. elegans-C. albicans infection model

The *C. elegans* infection model was carried out using previously described protocols (Muhammed et al., 2012). Briefly, 100 μL of overnight grown *C. albicans* was spread into a square lawn on a BHI plate containing kanamycin (45 μg/mL), followed by incubation for approximately 24 h at 30 °C. Approximately 400–500 synchronized adult *C. elegans glp-4; sek-1* nematodes were added to the center of the *C. albicans* lawns. The plates were incubated at 25 °C for 4 h. Worms were then carefully collected and washed with sterile M9. A total of 60–70 worms were then pipetted into a single well of a 12-well tissue culture plate containing 2 mL of liquid media (80% M9, 20% BHI, and 45 μg/mL kanamycin). Dead worms were removed and scored daily. Differences in the survival rates were determined using a log-rank test. Each experiment was performed at least in triplicate.

2.6. G. mellonella-C. albicans infection model

Last instar larvae of *G. mellonella* were placed in a Petri dish with a diameter of 10 cm. *C. albicans* strains were cultured in YPD liquid medium overnight at 30 °C with shaking at 200 rpm. The cells were collected by centrifugation, washed with sterile PBS, and then re-suspended in sterile PBS to a concentration of 2×10^8 colony-forming units/mL. Before the larvae was injected with *C. albicans*, the left lower foot of larvae should have been disinfected with 75% alcohol. Thereafter, the larvae were held by hand, and the yeast suspension (5 μL) was injected into the middle part of a larva with a Hamilton microinjection needle through the left lower foot. After injecting, the larvae were placed on a clean paper towel for 1 min before being transferred to a Petri plate for observation at 37℃. Dead larvae were removed every day, and the survival time was recorded. The percentage of survival was calculated, and the survival analysis was performed using the log-rank test (Li et al., 2013). Each experiment was performed at least in triplicate.

2.7. Ethics statement

The animal experiments were performed under the guidance of a protocol approved by the Animal Study Committee of the Institute of Dermatology, CAMS, according to the National Guidelines for Animal Care. All animal experiments were carried out with permission from the Ethical Committee of Institute of Zoonosis, the School of Pharmacy of Second Military Medical University, Shanghai, China.

2.8. Adhesion assay

The adhesion was visually observed (Nobile et al., 2006). The 24-well flat bottomed pre-sterilized microtiter plates were incubated with fetal bovine serum overnight at 37℃. A suspension of 1×10^7 cells of *C. albicans* in Spider medium was added to the wells and incubated at 37℃ for 2 h. Non-adherent cells were removed by washing with PBS. Fresh Spider medium was added to the corresponding wells and the plates were incubated at 37℃ for 24 h. The wells were washed and photographed. Each experiment was performed at least in triplicate.

2.9. Filamentation assay

A 1×10^6 cells/mL suspension of each strain in YPD, YPD + 10% FBS, Spider or Lee's liquid media was added to the wells of a 12-well flat-bottomed pre-sterilized microtiter plate and incubated at 37℃ for 2 h. The plates were visualized under inverted microscope and photographed. In addition, cells of each strain were serial diluted and spotted on YPD, YPD + 10% FBS, Spider, Lee's and SLAD agar, and incubated at 37℃ for 7 days. The colonies were photographed (Li et al., 2017). Each experiment was performed at least in triplicate.

2.10. Biofilm formation assay

The biofilms activity was assessed by XTT reduction assay, accordingly to previously described protocols (Peeters et al., 2008; Krom and Willems, 2017). *C. albicans* were cultured in YPD liquid medium overnight at 37℃ with shaking at 150 rpm. The cells were harvested by centrifugation, washed twice with a sterile PBS solution, and re-suspended in RPMI 1640 medium to prepare a suspension with the yeast cell concentration of 1×10^6 cells/mL. 100 μL of a suspension of *C. albicans* was added to the wells of 96-well flat bottomed pre-sterilized microtiter plates which were prepared with fetal bovine serum in advance and incubated at 37℃ for 90 min. Non-adherent cells were removed by washing with PBS. Fresh RPMI 1640 medium was added to the corresponding wells and the plates were incubated at 37℃ for 48 h. The suspension was removed by washing with PBS. 150 μL of XTT was added to the corresponding wells and the plates were incubated at 37℃ for 4 h. 70 μL of suspension was transferred to a new 96-well flat bottomed pre-sterilized microtiter plates and measured by microplate reader. Each experiment was performed at least in triplicate.

2.11. Cell surface hydrophobicity (CSH) and flocculation assay

A microbial adhesion test to hydrocarbon was used to measure the adhesion ability of each strain to a strongly hydrophobic cyclohexane and xylene medium (Klotz et al., 1985). *C. albicans* were cultured in YPD liquid medium overnight at 37℃ with shaking at 150 rpm. The cells were harvested by centrifugation, washed twice with a sterile PBS solution, and resuspended in PBS to prepare 3 mL of a suspension with the yeast cell concentration of OD_{600} = 1.0. After adding 150 μL of cyclohexane and xylene, the suspension was transferred to a glass test tube rinsed with an acidic solution. The mixture was incubated at 30℃ for 10 min, vortexed for 60 s, and then was allowed to stand at room temperature for 20 min for phase separation. For OD_{600} measurement, the aqueous phase at the bottom of the tube was quickly withdrawn with a sterile injection needle. The yeast suspension without the addition of cyclohexane and xylene was used as the negative control. CSH (%) was calculated as follows: (OD_{600}control - OD_{600}experiment)/OD_{600}control × 100%. Each experiment was repeated three times.

Flocculation was assayed by resuspending cells in RPMI 1640 media at an OD_{600} of 0.5, and incubating for 6 h at 37℃ with gentle shaking. Suspensions were vortexed for a few seconds and photographs of sedimenting cells were taken after 2 min.

2.12. Quantitative real time polymerase chain reaction (RT-qPCR) assay

Overnight cultures of tested strains in 5 mL of YPD at 30℃ were collected, then diluted into 100 mL of YPD or Spider medium to obtain an OD_{600} of 0.2 and incubated at 37℃ for additional 6 h. Total RNA was extracted using the E.Z.N.A. Yeast RNA kit (Omega Bio-tek) following the manufacturer's instruction. cDNA was synthesized and RT-qPCR was done as previously described (Guo et al., 2014). 18S rRNA was housekeeping gene for normalizing. The results were analyzed using the $2^{-\Delta\Delta CT}$ method, and statistical significance was determined using the one-way ANOVA test. The primer sequences of genes used in the RT-qPCR were showed in Table S2.

2.13. Determination of energy phenotypes using Xfe 96 seahorse assays

The Seahorse XF analyzer (XFe 96) was used to measure the oxygen consumption rate (OCR) and the extracellular acidification rate (ECAR). Exponentially grown yeast cells of all strains in YPD were washed twice with PBS, adjusted to 5×10^5 cells/well in 180 μL of assay medium, and then distributed into Poly-L-lysine (0.03%) XFe 96-well pre-coated microplates (Seahorse Bioscience) Three replicates of each strain or treated condition were used per experiment. All cell preparations in this assay medium were maintained in 96-well plates for 1 h at 30℃ to permit cell adhesion to the microtiter plates before analysis (Zhang et al., 2018a, 2018b). The two energy pathways (indicated by OCR and ECAR) of each strain were measured by the Seahorse XFe 96 as follows: baseline levels of both pathways were measured three times (5 min intervals) during the first 18 min at 30℃. In this phase, mitochondrial respiration is driven by 2 mM L-glutamine in the assay medium without glucose. Then, 10 mM glucose, 1.0 μM oligomycin, and 50 mM 2-deoxyglucose (2-DG) were sequentially injected automatically into assay wells. For each treatment, rates of OCR and ECAR were determined for six-time points at 40 min intervals. Oligomycin is a mitochondrial *etc*CV inhibitor that blocks the classical respiration chain (CRC) and stimulates ECAR in mammalian cells. 2-Deoxyglucose was used to inhibit glucose metabolism since it is a competitive inhibitor of the glucose hexokinase. Each experiment was performed at least in triplicate.

2.14. Mitochondrial function assay

All strains were grown in YPD overnight at 30°C. For determination of intracellular ATP concentrations, an aliquot of 1.0×10^6 cells from each strain was mixed with the same volume of BacTiter-GloTM reagent (Promega Corporation, Madison, WI, USA) and incubated for 5 min at room temperature as described previously (Zhang et al., 2012). ROS measurement was performed by using an oxidation-sensitive fluorescent dye DCFDA (Guo et al., 2014). Briefly, a suspension of 2.5×10^6 cells was stained with DCFDA (20 mg/mL) at 37°C for 20 min. The emission spectra at 488 nm and excitation spectra at 595 nm were determined by FACScan flow cytometer (Becton Dickinson). The cyanine dye JC-1 was used for determination of mitochondrial membrane potential of each strain (She et al., 2015). A suspension of 2.0×10^6 cells was incubated with 5 mmol/mL JC-1 at 37°C for 15 min and excitation spectra at 595 nm was determined by FACScan flow cytometer with emission spectra at 488 nm (Becton Dickinson).

2.15. NADH/NAD$^+$ ratio assay

For NADH/NAD$^+$ ratio calculation, all strains were grown in YPD at 30°C. Logarithmically growing cells were washed three times with pre-warmed sterile PBS. The NADH and NAD$^+$ contents were measured using NAD$^+$/NADH-Glo™ Assay (Promega Corporation, Madison, WI). Luminescent signals were determined on a full wavelength multi-functional enzyme mark instrument (Thermo Scientific). NADH/NAD$^+$ ratio was calculated. All experiments were performed in triplicate on two separate days. *P*-values were determined using the unpaired Student's *t*-test.

3. Results

3.1. ADH1 deletion has only a minor effect on C. albicans growth

Growth curves are plotted from several kinetics experiments and doubling time (DT) is calculated to investigate the effect of the *ADH1* deletion on the growth of *C. albicans*. We find that all experimental strains entered the logarithmic growth phase at 6 h and the stationary phase at 12 h of growth (Fig. 1A) and the constituted strain *adh1Δ/ADH1* and SC5314 are not significantly different in growth either in growth curve or spot assays. Compared with SC5314, the *adh1Δ/Δ* strain shows little difference in DT during the logarithmic growth phase ($P > 0.05$) (Fig. 1C). Similar growth patterns are found in the spot assay as well, and we find that the cell viability of *adh1Δ/Δ* strain is similar to SC5314 in glucose (Fig. 1B) and slightly reduced in non-fermentable carbon sources such as glycerol, ethanol, oleic acid and citrate ($P > 0.05$, Fig. S6). These results indicate that *ADH1* has only a minor effect on *C. albicans* growth.

3.2. ADH1 deletion reduces the pathogenicity of C. albicans in vivo

A mouse model of hematogenously disseminated candidiasis is first used to measure the virulence of *adh1Δ/Δ in vivo*, which is the standard for investigating the pathogenesis of this disease (Spellberg et al., 2005). The *adh1Δ/Δ*-infected mice have a significantly higher survival rate when compared with SC5314-infected mice ($P < 0.05$) (Fig. 2A). Also, the *adh1Δ/Δ*-infected mice have a significantly lower fungal burden in the liver and kidneys compared with that of SC5314-infected mice ($P < 0.05$) (Fig. 2B); kidney histopathological sections of the SC5314- and *adh1Δ/ADH1*-infected mice showed high inflammatory cell infiltration and many agglomerated hyphae by Periodic Acid-Schiff staining, while the kidneys of the *adh1Δ/Δ*-infected mice had no obvious tissue damage and no hyphae agglomerate formation (Fig. 2C). The phenotypes of *adh1Δ/ADH1* are the same as those of SC5314 (Fig. 2A–C).

To determine further if *ADH1* is involved in virulence, the *C. albicans* strains are used to infect two invertebrate hosts (*C. elegans* and *G. mellonella*) which lack adaptive immunity (McClelland et al., 2016). Consistent with the findings in mice, the *adh1Δ/Δ*-infected *C. elegans* and *G. mellonella* showed a significantly prolonged survival time compared with those of the SC5314-infected *C. elegans* and *G. mellonella,* respectively ($P < 0.05$) (Fig. 2E and F); the phenotype of *adh1Δ/ADH1* is the same as that of SC5314.

Next, to determine whether *ADH1* virulence effects are due to morphological differences, we quantify the proportion of *C. elegans* with filamentous *C. albicans* that can be observed, as the pathogenesis of *C. elegans* infection system depends on hyphal morphogenesis (McClelland et al., 2016; Pukkila-Worley et al., 2009; Graham et al., 2017). We find that the *adh1Δ/Δ*-infected *C. elegans* shows a dramatic decrease in the number of worms with filamentous *C. albicans*, showing clear evidence of invasive fungal hyphae relative to SC5314-infected *C. elegans* (Fig. 2D); the phenotype of *adh1Δ/ADH1* is the same as that of SC5314.

Taken together, these results indicate that *ADH1* contributes to the pathogenicity of *C. albicans* likely *via*promotion of hyphal formation.

3.3. ADH1 deletion reduces the adhesion ability of C. albicans

Adhesion assay reveals that *adh1Δ/Δ* fails to adhere to the bottom of the microtiter plate when compared with SC5314 and *adh1Δ/ADH1* (Fig. 3A). At the same time, the adhesive-specific genes (*ALS1* and *ALS3*) in RT-qPCR assay are markedly down-regulated in the *adh1Δ/Δ* when compared with SC5314 and *adh1Δ/ADH1* ($P < 0.05$) (Fig. 3B). These results indicate that *ADH1* may be related to the adhesion process in *C. albicans*.

3.4. ADH1 deletion displays defective filamentation

Filamentous growth enables *C. albicans* to penetrate tissue and avoid host immune cells after endocytosis (Dalle et al., 2010; Zhu and Filler, 2010). In hyphal-inducing media, the *adh1Δ/Δ* displays shorter or even pseudohyphae compared with SC5314 and *adh1Δ/ADH1*, which show long and massive filamentous growth under microscopy (Fig. 4A). Similar results are seen on hyphae-inducing agar media. The *adh1Δ/Δ* displays a more severe defective phenotype in filamentous growth and

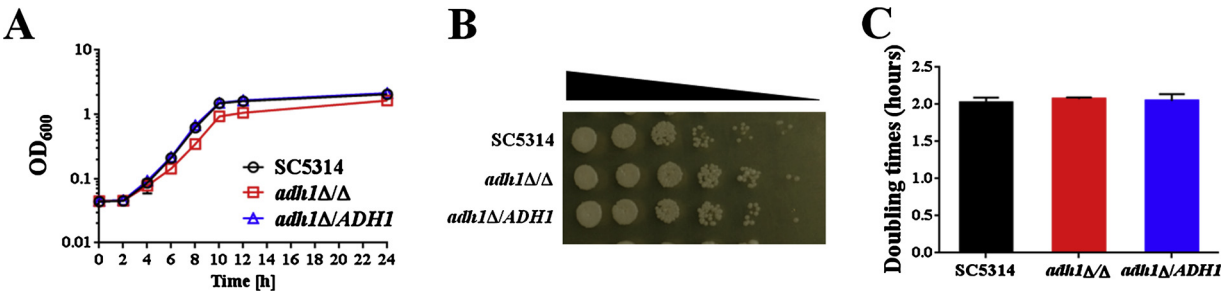

Fig. 1. Deletion of *ADH1* has only a minor effect on *C. albicans* growth. A, growth curves; B, spot assay (used to measure cell viability); C, doubling times of *C. albicans strains* in the exponential growth phase. Representative results from three experiments are shown. The results are mean ± SD values.

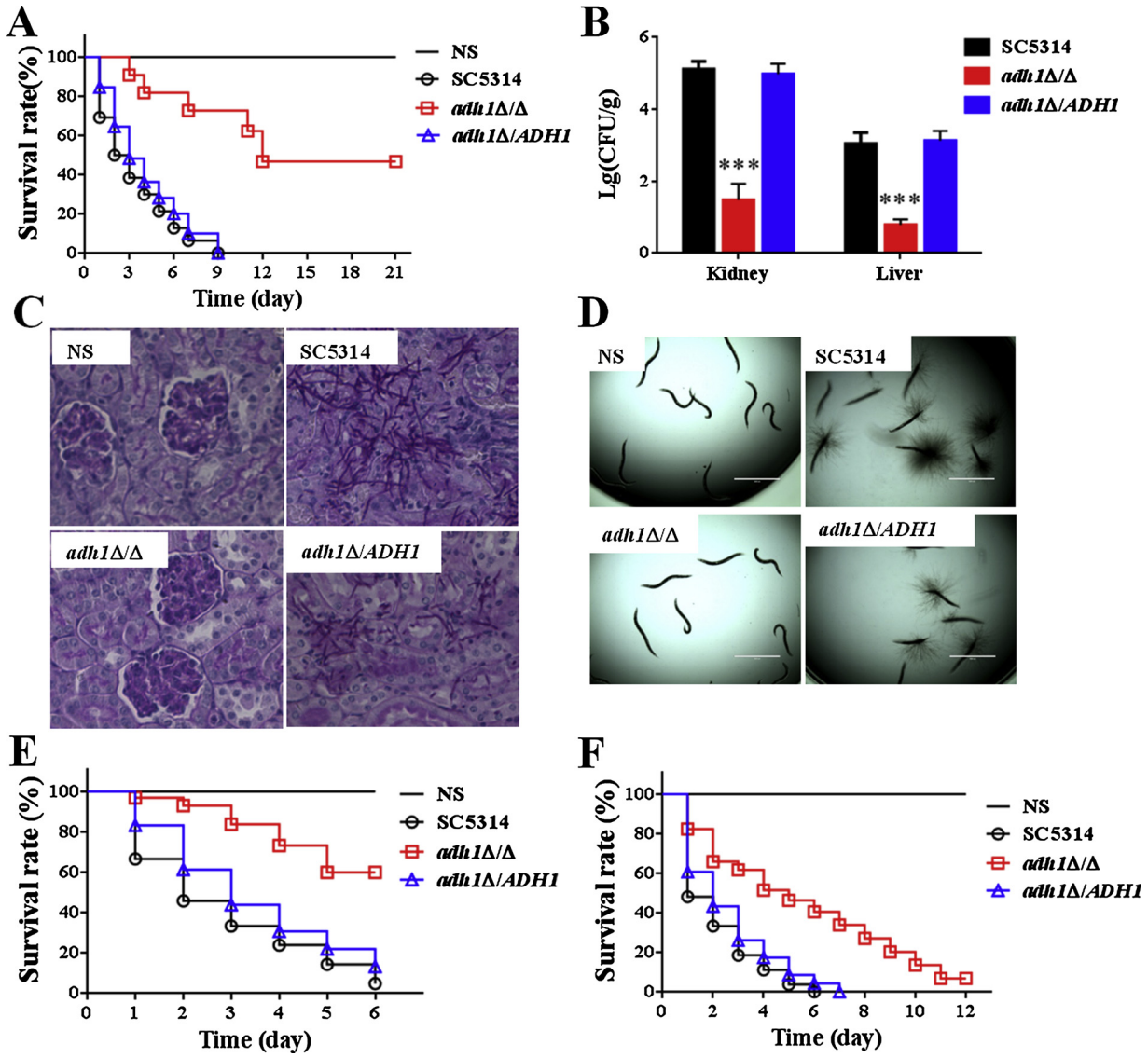

Fig. 2. Deletion of *ADH1* reduces the virulence of *C. albicans* infection *in vivo*. A, survival curves of mice infected with different *C. albicans* strains; B, fungal burden of mice infected with different *C. albicans* strains; C, histopathological analysis of mice infected with different *C. albicans* strains (PAS, ×200); D, the evidence of visible *C. albicans* filaments penetrating the *C. elegans* cuticle after 2 d of infection (×200); E, survival curves of *C. elegans* infected with different *C. albicans* strains; F, survival curves of *G.mellonella* infected with different *C. albicans strains*. NS group was the mice treated with saline as a control. Representative results from three experiments are shown. The results are mean ± SD values. *** $P < 0.001$ *vs*SC5314.

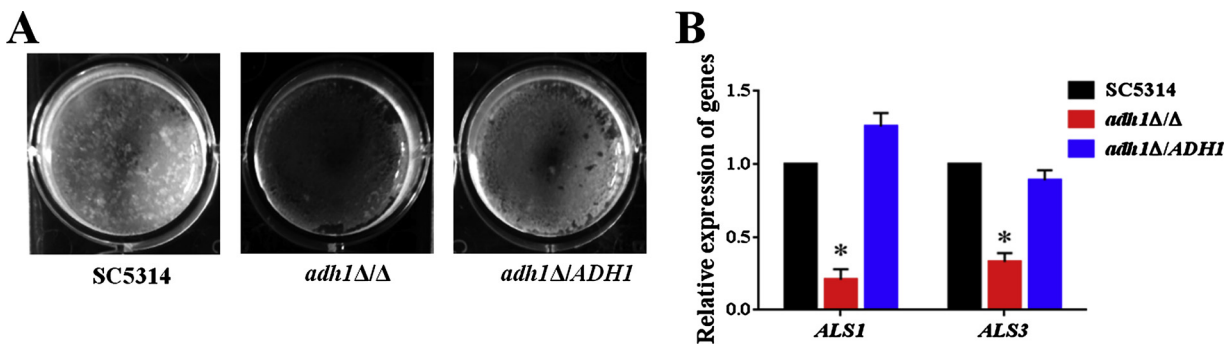

Fig. 3. Deletion of *ADH1* confers defective adhesion. A, effect of *ADH1* on *C. albicans* adhesion. 1×10^7 cells suspension of *C. albicans* in spider was added to 24-well flat-bottomed plates and incubated for 24 h at 37°C. The wells were washed with PBS and taken photos. B, effect of *ADH1* on the expression of *C. albicans* adhesion genes. Representative results from three experiments are shown. The results are mean ± SD values. * $P < 0.05$ *vs*SC5314.

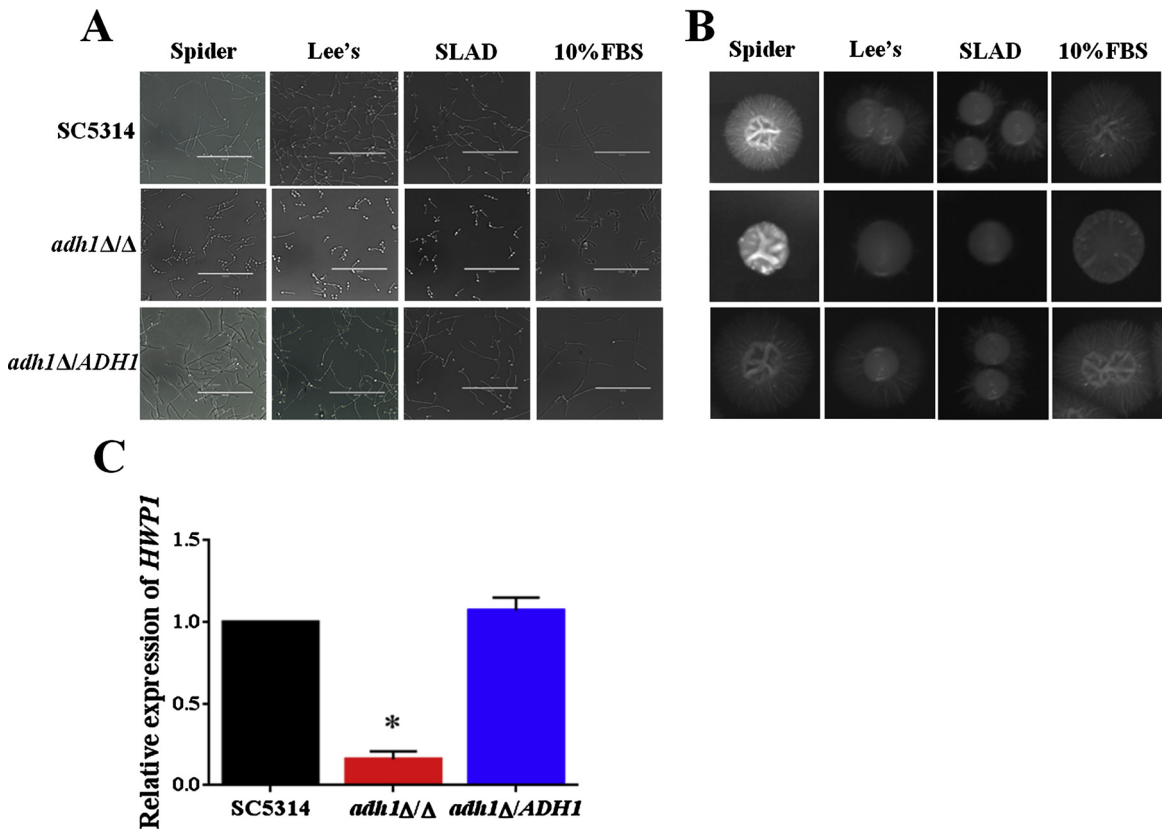

Fig. 4. Deletion of *ADH1* confers defective filamentation and colony formation. A, overnight cultures of the strains were resuspended to 1.0×10^6 cells/mL, and added into 12-well microtiter plates with filaments-inducing media. All the plates were cultured at 37℃ for 2 h before photographed. B, overnight cultures of the strains were resuspended, and 500 cells were spotted onto the indicated filaments-inducing agar plates. All the plates were cultured at 37℃ for 7 days before photographed. C, effect of *ADH1* on the expression of *C. albicans* hyphal-specific gene were determined by RT-qPCR. Representative results from three experiments are shown. The results are mean ± SD values. * $P < 0.05$ *vs*SC5314.

even forms smooth colonies due to the lack of peripheral and invasive filaments, while SC5314 and *adh1Δ/ADH1* produce large colonies with florid and invasive filaments on the edges (Fig. 4B). The defective filamentation in the *adh1Δ/Δ* is consistent with marked down-regulation of hyphal-specific genes such as *HWP1* in RT-qPCR assay (Fig. 4C). These *in vitro* results again emphasize that *ADH1* is required for the filamentation process in *C. albicans*.

3.5. ADH1 deletion reduces metabolic activity during biofilm formation

Aside from filament propensity, biofilm also carries important clinical consequences because it will shield organisms from most antifungal therapies and therefore withstand host immune defenses (Nett et al., 2010). The metabolic activity of the *adh1Δ/Δ* during biofilm formation is obviously reduced compared with that of SC5314 ($P < 0.001$) in XTT assay; however, the metabolic activity of the *adh1Δ/ADH1* in biofilm formation process is the same with that of SC5314 ($P > 0.05$) (Fig. 5).

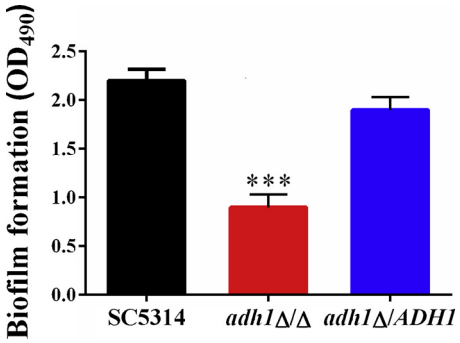

Fig. 5. *In vitro* biofilm formation assay of *C. albicans* strains. Strains were cultured in RPMI-1640 medium. After 48-h incubation, the biofilm biomass was quantitated using the XTT assay. Representative results from three experiments are shown. The results are mean ± SD values. *** $P < 0.001$ *vs*SC5314.

3.6. ADH1 deletion enhances CSH and flocculation of C. albicans

Cell surface hydrophobicity has also been shown to be closely related to pathogenicityof *C. albicans* (Rodrigues et al., 1999). We find that *ADH1* deletion enhances the hydrophobicity and flocculation of *C. albicans,* demonstrating significantly higher CSH in *adh1Δ/Δ* strain when compared with SC5314 ($P < 0.01$) and *adh1Δ/ADH1* (Fig. 6A). Consistent with the CSH result, *adh1Δ/Δ* mutant shows increased flocculation compared to SC5314 and the *adh1Δ/ADH1* strain (Fig. S7). However, the RT-qPCR results shows that the expression of a CSH-associated gene (*CSH1*) in *adh1Δ/Δ* is significantly downregulated compared with SC5314 ($P < 0.05$) as the expression of *CSH1* in *adh1Δ/ADH1* is the same with that of SC5314 ($P > 0.05$) (Fig. 6B).

3.7. Effects of the ADH1 deletion on glycolysis and mitochondrial oxygen consumption in C. albicans

To determine the effect of *ADH1* on *C. albicans* bioenergetics, ECAR (extracellular acidification rate) and OCR (oxygen consumption rate) are measured in real time as respective markers of glycolysis and oxidative phosphorylation in glycolytic assay using extracellular flux (XF) analysis technology. The results show that the basal ECAR, glycolysis, glycolytic capacity, and glycolytic reservoir in the *adh1Δ/Δ* are not

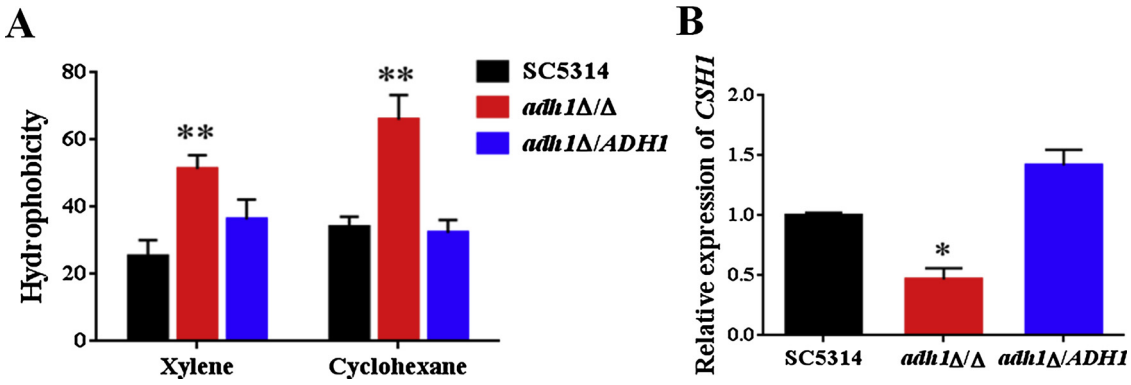

Fig. 6. Deletion of *ADH1* displays increased cell surface hydrophobicity (CSH). A, overnight cultures of the strains were cultured in YPD media for 48 h. CSH of *C. albicans* was measured by water-hydrocarbon two-phase assay. B, effect of *ADH1* on the expression of *C. albicans* CSH gene were determined by RT-qPCR. Representative results from three experiments are shown. The results are mean ± SD values. * $P < 0.05$, ** $P < 0.01$ *vs*SC5314.

significantly different when compared with those of SC5314 ($P > 0.05$) while the *adh1Δ/ADH1* is similar to SC5314 in these parameters ($P > 0.05$) (Fig. 7A, B). Therefore, the *ADH1* deletion has only a minor effect on *C. albicans* glycolysis.

However, the measurement of oxygen consumption rates (OCR), which operate primarily in mitochondria, reveals a 2-fold increase in the basal respiration of the *adh1Δ/Δ* mutant compared with that of the SC5314, which is statistically significant ($P < 0.05$). Meanwhile, the OCR of *adh1Δ/ADH1* is similar to that of SC5314 ($P > 0.05$) (Fig. 7C, D). Together with ECAR result, the metabolic phenotype of *adh1Δ/Δ* mutant is to stimulate mitochondrial oxygen consumption without inhibiting glycolysis in *C. albicans*.

3.8. Deletion of ADH1 results in a suppression of mitochondrial activity

With a higher OCR in *adh1Δ/Δ* mutant, we next analyse other mitochondrial activities such as the intracellular ATP content. Regardless OCR elevation, we found that the intracellular ATP concentration of *adh1Δ/Δ* drops by more than 50% of SC5314 level ($P < 0.0001$) (Fig. 8A) and the membrane potential of the *adh1Δ/Δ* is significantly decreased compared to the level of SC5314 ($P < 0.001$) (Fig. 8B). Meanwhile, we found that *adh1Δ/Δ* has an increased ROS level when compared with that of SC5314 ($P < 0.05$) (Fig. 8C). The *adh1Δ/ADH1* was similar to SC5314 ($P > 0.05$). These data suggest a critical role for *ADH1* in mitochondrial function, which may explain the defective

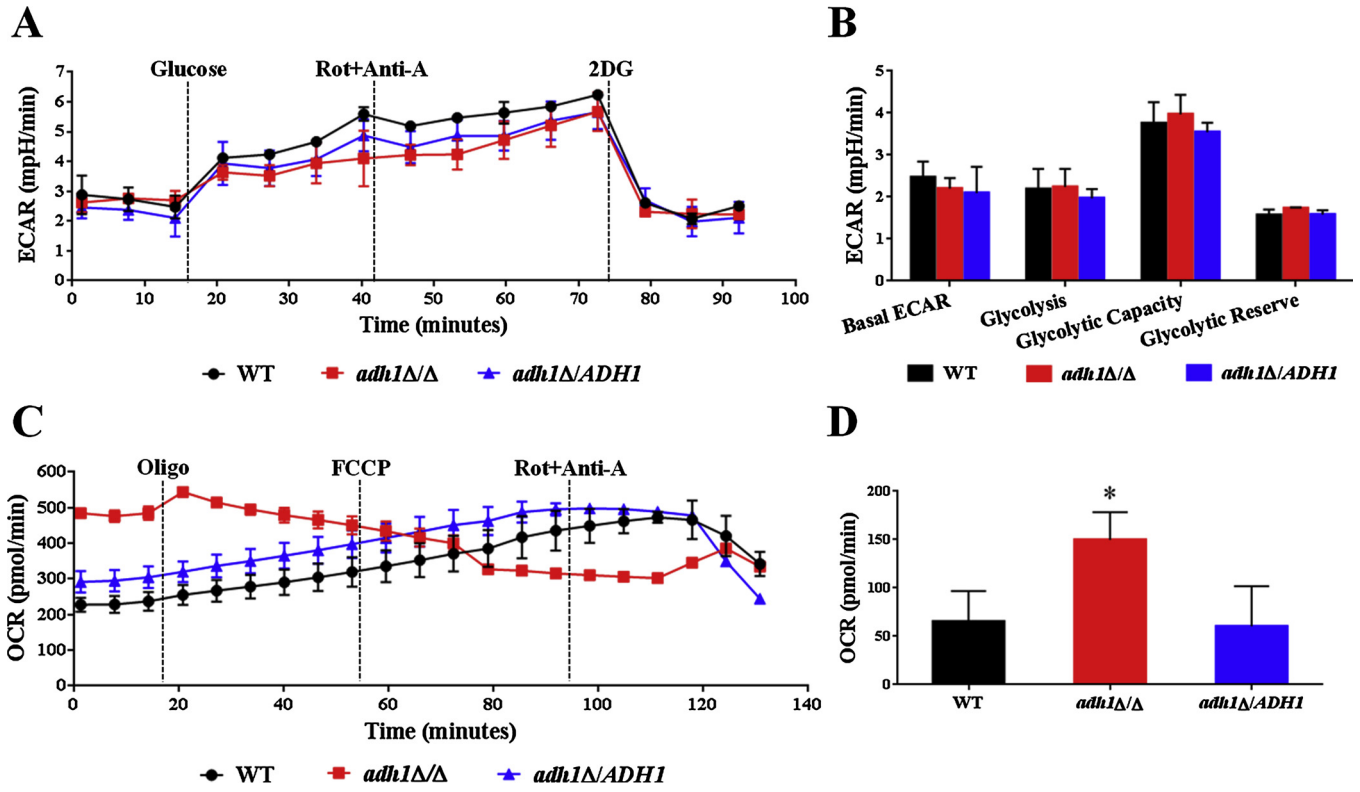

Fig. 7. *ADH1* affects the metabolic fate of *C. albicans*. The activity and integrity of glycolysis and mitochondrial respiration in *C. albicans* cells were determined by extracellular flux analysis. A, glycolysis was studied by analyzing extracellular acidification rates (ECAR) after sequential additions of glucose (10 mM), rotenone (Rot, 0.5 μM) and antimycin A (Anti-A, 0.5 μM) and 2-deoxyglucose (2DG, 50 mM); B, quantification of the glycolysis data obtained in A; C, mitochondrial respiration was assessed by measuring oxygen consumption rates (OCR) after sequential addition of oligomycin (Oligo, 10 μM), CCCP (2 μM), rotenone (Rot, 0.5 μM) and antimycin A (Anti-A, 0.5 μM); D, quantification of the mitochondrial respiration data obtained in C. The results are shown as the average of four independent experiments. The results are mean ± SD values. *$P < 0.05$ *vs*SC5314.

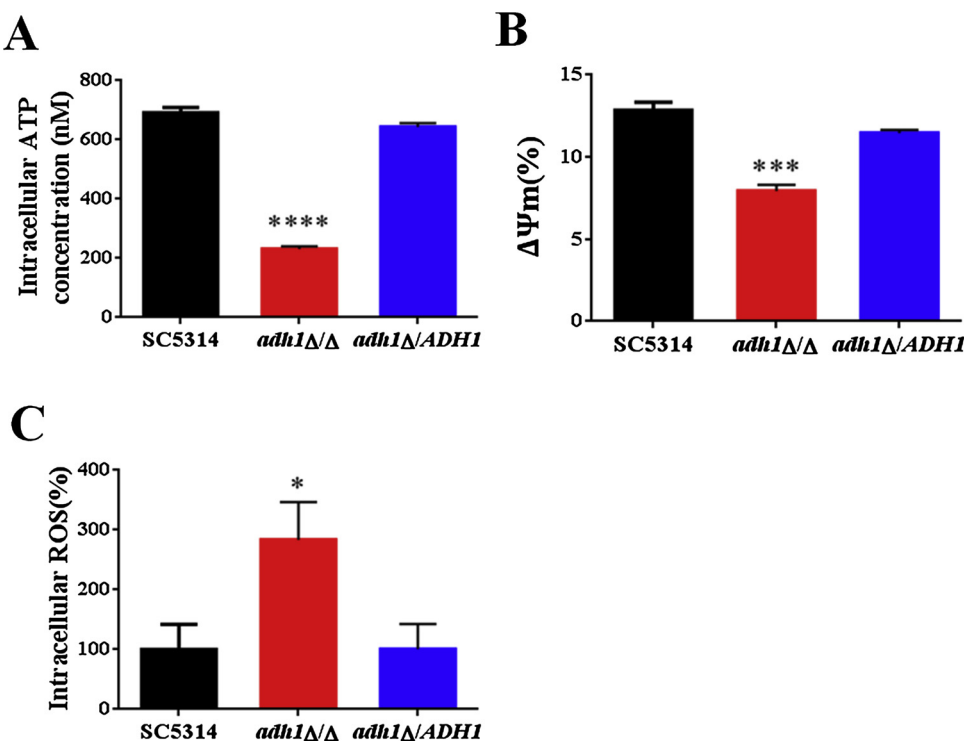

Fig. 8. Deletion of *ADH1* results in decreasing mitochondrial activity. A, the intracellular ATP content was measured by microplate reader. B, mitochondrial membrane potential was measured with JC-1 dye by flow cytometry. C, the ROS levels were measured with DCFDA dye by flow cytometry. Representative results from three experiments are shown. The results are mean ± SD values. * $P < 0.05$, *** $P < 0.001$, **** $P < 0.0001$ *vs*SC5314.

filamentation in the mutant as noted above, since the association of mitochondrial activity with *C. albicans* filamentation has been observed previously (Bambach et al., 2009; Grahl et al., 2015).

3.9. Deletion of ADH1 results in increasing NADH/NAD$^+$ ratio

As NAD$^+$ regeneration during acetaldehyde reduction is a key step of glycolytic continuity, we assess the impact of *ADH1* on *C. albicans* NADH/NAD$^+$ redox balance. NADH is a central redox cofactor of the living cells that is incorporated in mitochondrial electron transport chain and in cytosol alcohol oxidation for energy production. We find that NADH/NAD$^+$ ratio increased in *adh1*Δ/Δ mutant when compared with SC5314 and the *adh1*Δ/*ADH1* strain ($p < 0.05$) (Fig. S8). The change of the intracellular NADH/NAD$^+$ redox in *adh1*Δ/Δ mutant likely is caused by a blockage of acetaldehyde into alcochol, which again confirms that Adh1p in *C. albicans* is responsible for converting acetaldehyde into alcohol (Mukherjee et al., 2006; Chen et al., 2014; Zhang et al., 2018a, 2018b).

4. Discussion

The pathogenic roles of Adh1p in candidiasis were noted but not systematically studied. The earlier studies of Adh1p function in microorganisms such as *C. albicans* focused on its catalytic roles in ethanol and acetaldehyde metabolism in cytosol (Thomson et al., 2005; Mukherjee et al., 2006; Chen et al., 2014; Zhang et al., 2018a, 2018b). The involvement of Adh1p of *C. albicans* in mitochondrial oxidative phosphorylation as we observed in this study is seldom described. In this study, we first construct *ADH1* deletion mutant and revertant strains by *SAT1* flipper strategy. The effects of *ADH1* deletion on the pathogenicity of *C. albicans* are then determined both *in vitro* and *in vivo* when compared to each phenotype of parental strain SC5314.

We use three host model systems with different immune responses - ICR mice, *C. elegans* and *G. mellonella* -to evaluate the effects of *ADH1* deletion on the pathogenicity of *C. albicans in vivo*. We find that the *adh1*Δ/Δ-infected mice are generally in a better condition with a significantly prolonged survival time. The pathological examination of the *adh1*Δ/Δ-infected mice shows fungal burden in the liver and kidney and tissue damage are less than that of SC5314 and *adh1*Δ/*ADH1*. Consistent with this, survival times for the mutant strain are also significantly longer than for SC5314 and *adh1*Δ/*ADH1* in the two non-mammalian models *C. elegans* and *G. mellonella*. These results demonstrate that *ADH1* promotes the pathogenicity of *C. albicans*. Given that growth curves and spot assays *in vitro* show that *ADH1* deletion has only a minor effect on the growth and cell viability of *C. albicans*, it seems clear that the attenuated pathogenicity is unlikely to have been caused by the slow growth.

Hyphal formation has long been associated with *C. albicans* colonization and invasion of host tissues (Lo et al., 1997), which is defective in *adh1*Δ/Δ-infected mice while invasive hyphal formation is easily found in the kidneys of SC5314- and *adh1*Δ/*ADH1*-infected mice. Furthermore, in the nematode infection system where pathogenesis depends greatly on hyphal morphogenesis (Pukkila-Worley et al., 2009; Graham et al., 2017), the number of worms with invasive fungal hyphae in *adh1*Δ/Δ-infected *C. elegans* is fewer than in SC5314- and *adh1*Δ/*ADH1*-infected worms. Consistent with the *in vivo* results, the *adh1*Δ/Δ shows short filaments and smooth colonies and a lack of peripheral and invasive filaments *in vitro*. Therefore, failure to form hyphae in *ADH1* deletion mutant contributes to this pathogenic phenotype.

Both virulence factors of *C. albicans* and the host immune defense impact the pathogenesis of *C. albicans*. Hyphal formation is a key virulence factor (Lo et al., 1997) and is also crucial for biofilm formation (Ramage et al., 2002). The reduced pathogenicity of mutant *in vivo* is accompanied by defective hyphal formation, decreased adhesion, and reduced metabolic activity during biofilm formation. Meanwhile the virulence-related genes such as *ALS1*, *ALS3*, *HWP1*, and *CSH1* are accordingly down-regulated in *adh1*Δ/Δ strain compared with that of SC5314 and *adh1*Δ/*ADH1*. These results further indicate that *ADH1* contributes to the pathogenicity of *C. albicans via* these virulence factors.

In contrast to down-regulated *CSH1*, *ADH1* deletion enhances cell surface hydrophobicity that may be important for cell dispersal during invasive infection and possibly for morphological development. This result was also shown by Gelis et al. (Gelis et al., 2012), they reported that increasing surface hydrophobicity is consistent with reduced virulence in a mouse model of disseminated candidiasis. Our CSH result

is negatively correlated to adhesion. The influence of CSH on adhesion of microorganisms to biotic and abiotic surfaces in medicine as well as in bioremediation and fermentation industry has both negative and positive aspects (Krasowska and Sigler, 2014). Theoretically, the more hydrophobic cells adhere more strongly to hydrophobic polystyrene microtiter plate surfaces. However, in the planktonic culture freely living microorganism is possible to present as hydrophilic and hydrophobic cells, but only part of them participate in the adhesion; Also, microorganism can switch between hydrophobic and hydrophilic phenotypes in response to changes in environmental conditions (temperature, composition of nutrients, *etc.)* and growth phases (Borecká-Melkusová and Bujdáková, 2008; Bujdakova et al., 2013; Krasowska and Sigler, 2014; Singleton et al., 2001). The testing condition in CSH assay in this study is *C. albicans* resuspended in PBS and incubated at room temperature for 20 min, but adhesion assay was performed by *C. albicans* resuspended in Spider medium and incubated at 37°C for 24 h. The difference of CSH and the mRNA expression of *CSH1* can be explained by the experiment conditions as given here. RT-qPCR assay of *CSH1* agrees as to the conditions for adhesion and biofilm formation assay but different from that of CSH assay.

In accordance with our findings with *C. albicans*, Finelli et al. (Finelli et al., 2003) showed that disruption of a putative *Pseudomonas aeruginosa* alcohol dehydrogenase had no effect on planktonic growth but caused defects in biofilm formation in static and flowing systems. Also*, ADH1* deletion decreased *Fusarium oxysporum* virulence (Corrales Escobosa et al., 2011). In contrast to reduced XTT activity in *C. albicans* biofilm in this study, Mukherjee et al. (Mukherjee et al., 2006) reported that *ADH1* deletion resulted in enhancing *C. albicans* biofilm formation and metabolic activity through decreasing ethanol. This contrary result may have several explanations: the parental strain for comparison, the genetic background of *adh1*Δ/Δ construction, or even the medium used for biofilm formation assay. All these differ completely from those employed by Mukherjee et al., but we find the following explanation more compelling: increasing acetaldehyde itself, which also results from *ADH1* deletion, has reported to inhibit biofilm formation (Mukherjee et al., 2006; Chauhan et al., 2011). The contradictory effects of decreased ethanol and increased acetaldehyde on *C. albicans* biofilm formation from *ADH1* deletion then deserves further study.

The association of *C. albicans* filamentation with mitochondrial activity has been noted previously (Bambach et al., 2009; Grahl et al., 2015). For bioenergetic roles of *ADH1* in *C. albicans*, we find that intracellular ATP content in the *adh1*Δ/Δ is significantly decreased along with significantly decreased mitochondrial membrane potential when compared with SC5314 or *adh1*Δ/*ADH1*. The increased/decreased intracellular ATP content activates/inhibits the cAMP/PKA signalling pathway which regulates *C. albicans* virulence factors (Inglis and Sherlock, 2013; Grahl et al., 2015; Tao et al., 2017). The attenuating pathogenicity in *adh1*Δ/Δ is probably due to a decrease in intracellular ATP content, which suppresses the cAMP-PKA signalling pathway to inhibit the multiple virulence factors.

The intracellular ATP required for the growth, reproduction, virulence of *C. albicans* is mainly generated by glycolysis and oxidative phosphorylation. The oxidative phosphorylation in mitochondria accounts for about 90% of intracellular ATP (Vander Heiden et al., 2009). Since Adh1p is an important enzyme related to glycolysis, we investigated the effects of the *ADH1* deletion in *C. albicans* glycolysis as well. The Xfe 96 seahorse assays show that the *adh1*Δ/Δ did not exhibit any significant effect on glycolysis but has a significantly higher mitochondrial OCR than SC5314 or *adh1*Δ/*ADH1*. Mitochondrial function studies show that ROS levels are significantly increased in the *adh1*Δ/Δ strain. Since a high OCR and decreased ATP production are observed in *ADH1* deletion mutant, ROS elevation therefore could be partially explained by conversion of large quantities of O_2 directly to ROS instead of H_2O. The increased OCR in *ADH1* deletion mutant could be explained by an increase in futile proton conductance that leads to membrane depolarization, as seen with classic uncouplers. Therefore, *ADH1* deletion may somehow promote the 'uncoupling event'.

Consistent with increasing OCR, we find that *adh1*Δ/Δ increases the reducing equivalents (NADH/NAD^+), which may be due to decreased NAD^+ during acetaldehyde to ethanol conversion. However, ATP reduction may stimulate glycolysis and TCA that then increases the NADH. It has been shown that, in the case of *E. coli* and *C. glutamicum*, ATP depletion increased production of reducing equivalents, which entered the electron transport chain and increased oxygen consumption (Holm et al., 2010; Sekine et al., 2001). We believe that the increased reducing equivalents in *C. albicans adh1*Δ/Δ would use the same mechanism to accelerate the activity of mitochondrial and oxygen consumption.

In summary, we find that *ADH1* deletion inhibits mitochondrial oxidative phosphorylation and hyphal formation in *C. albicans*. Because of the decreased intracellular ATP content, the suppression of the cAMP-PKA signalling pathway inhibits the multiple virulence factors that ultimately attenuate *C. albicans* pathogenicity.

Author contributions

Yanjun Song, Shuixiu Li, Yajing Zhao, Yishan Zhang, Hong Zhang were involved in study design. Yanjun Song, Shuixiu Li, Yajing Zhao, Yishan Zhang executed the experiments. Yanjun Song, Shuixiu Li, Yajing Zhao, Yishan Zhang, Yan Lv, Yuanying Jiang, Yan Wang, Dongmei Li, Hong Zhang performed the data analyses and writing. All authors read and approved the final manuscript.

Funding

This work was supported by the National Natural Science Foundation of China (81471995/81171542) and China Postdoctoral Science Foundation (2019M653291).

Declaration of Competing Interest

The authors declare no conflict of interest.

Appendix A. Supplementary data

Supplementary material related to this article can be found, in the online version, at doi:https://doi.org/10.1016/j.ijmm.2019.151330.

References

Bambach, A., Fernandes, M.P., Ghosh, A., Kruppa, M., Alex, D., Li, D., Fonzi, W.A., Chauhan, N., Sun, N., Agrellos, O.A., Vercesi, A.E., Rolfes, R.J., Calderone, R., 2009. Goa1p of *Candida albicans* localizes to the mitochondria during stress and is required for mitochondrial function and virulence. Eukaryot. Cell 8, 1706–1720.

Becker, P., Hufnagle, W., Peters, G., Herrmann, M., 2001. Detection of differential gene expression in biofilm-forming versus planktonic populations of *Staphylococcus aureus* using micro-representational-difference analysis. Appl. Environ. Microbiol. 67 (7), 2958–2965.

Bertram, G., Swoboda, R.K., Gooday, G.W., Gow, N.A., Brown, A.J., 1996. Structure and regulation of the *Candida albicans ADH1* gene encoding an immunogenic alcohol dehydrogenase. Yeast 12 (2), 115–227.

Borecká-Melkusová, S., Bujdáková, H., 2008. Variation of cell surface hydrophobicity and biofilm formation among genotypes of *Candida albicans* and *Candida dubliniensis* under antifungal treatment. Can. J. Microbiol. 54 (9), 718–724.

Bujdakova, H., Didiasova, M., Drahovska, H., Cernakova, L., 2013. Role of cell surface hydrophobicity in *Candida albicans* biofilm. Cent. Eur. J. Biol. 8, 259–262.

Chauhan, N.M., Raut, J.S., Karuppayil, S.M., 2011. Acetaldehyde inhibits the yeast-to-hypha conversion and biofilm formation in Candida albicans. Mycoscience 52 (5), 356–360.

Chen, A.I., Dolben, E.F., Okegbe, C., Harty, C.E., Golub, Y., Thao, S., Ha, D.G., Willger, S.D., O'Toole, G.A., Harwood, C.S., Dietrich, L.E., Hogan, D.A., 2014. *Candida albicans* ethanol stimulates Pseudomonas aeruginosa WspR-controlled biofilm formation as part of a cyclic relationship involving phenazines. PLoS Pathog. 10 (10), e1004480.

Corrales Escobosa, A.R., Rangel Porras, R.A., Meza Carmen, V., Gonzalez Hernandez, G.A., Torres Guzman, J.C., Wrobel, K., Wrobel, K., Roncero, M.I., Gutierrez Corona, J.F., 2011. *Fusarium oxysporum* Adh1 has dual fermentative and oxidative functions and is involved in fungal virulence in tomato plants. Fungal Genet. Biol. 48 (9),

886–895.
Crowe, J.D., Sievwright, I.K., Auld, G.C., Moore, N.R., Gow, N.A., Booth, N.A., 2003. *Candida albicans* binds human plasminogen: identification of eight plasminogen-binding proteins. Mol. Microbiol. 47 (6), 1637–1651.
Dalle, F., Wächtler, B., L'Ollivier, C., Holland, G., Bannert, N., Wilson, D., Labruère, C., Bonnin, A., Hube, B., 2010. Cellular interactions of *Candida albicans* with human oral epithelial cells and enterocytes. Cell. Microbiol. 12, 248–271.
Finelli, A., Gallant, C.V., Jarvi, K., Burrows, L.L., 2003. Use of in-biofilm expression technology to identify genes involved in *Pseudomonas aeruginosa* biofilm development. J. Bacteriol. 185 (9), 2700–2710.
Gelis, S., de Groot, P.W., Castillo, L., Moragues, M.D., Sentandreu, R., Gómez, M.M., Valentín, E., 2012. Pga13 in *Candida albicans* is localized in the cell wall and influences cell surface properties, morphogenesis and virulence. Fungal Genet. Biol. 49 (4), 322–331.
Gillum, A.M., Tsay, E.Y., Kirsch, D.R., 1984. Isolation of the *Candida albicans* gene for orotidine-5′-phosphate decarboxylase by complementation of *S. cerevisiae* ura3 and *E. coli* pyrF mutations. Mol. Gen. Genet. 198, 179–182.
Graham, C.E., Cruz, M.R., Garsin, D.A., Lorenz, M.C., 2017. *Enterococcus faecalis* bacteriocin EntV inhibits hyphal morphogenesis, biofilm formation, and virulence of *Candida albicans*. Proc. Natl. Acad. Sci. U. S. A. 114 (17), 4507–4512.
Grahl, N., Demers, E.G., Lindsay, A.K., Harty, C.E., Willger, S.D., Piispanen, A.E., Hogan, D.A., 2015. Mitochondrial activity and Cyr1 are key regulators of Ras1 activation of *C. albicans* virulence pathways. PLoS Pathog. 11, e1005133.
Guo, H., Xie, S.M., Li, S.X., Song, Y.J., Lv, X.L., Zhang, H., 2014. Synergistic mechanism for tetrandrine on fluconazole against *Candida albicans* through the mitochondrial aerobic respiratory metabolism pathway. J. Med. Microbiol. 63, 988–996.
Hazelwood, L.A., Daran, J.M., van Maris, A.J., Pronk, J.T., Dickinson, J.R., 2008. The Ehrlich pathway for fusel alcohol production:a century of research on Saccharomycescerevisiae metabolism. Appl. Environ. Microbiol. 74 (8), 2259–2266.
Holm, A.K., Blank, L.M., Oldiges, M., Schmid, A., Solem, C., Jensen, P.R., Vemuri, G.N., 2010. Metabolic and transcriptional response to cofactor perturbations in Escherichia coli. J. Biol. Chem. 285 (23), 17498–17506.
Inglis, D.O., Sherlock, G., 2013. Ras signaling gets fine-tuned: regulation of multiple pathogenic traits of *Candida albicans*. Eukaryot. Cell 12 (10), 1316–1325.
Klotz, S.A., Drutz, D.J., Zajic, J.E., 1985. Factors governing adherence of *Candida* species to plastic surfaces. Infect. Immun. 50 (1), 97–101.
Klotz, S.A., Pendrak, M.L., Hein, R.C., 2001. Antibodies to alpha5beta1 and alpha(v)beta3 integrins react with *Candida albicans* alcohol dehydrogenase. Microbiology 147 (Pt 11), 3159–3164.
Krasowska, A., Sigler, K., 2014. How microorganisms use hydrophobicity and what does this mean for human needs? Front. Cell. Infect. Microbiol. 4, 112.
Krom, B.P., Willems, H.M., 2017. *In vitro* models for *Candida* biofilm development. Methods Mol. Biol. 1356, 95–105.
Kwak, M.K., Ku, M., Kang, S.O., 2014. NAD(+)-linked alcohol dehydrogenase 1 regulates methylglyoxal concentration in *Candida albicans*. FEBS Lett. 588 (7), 1144–1153.
Leskovac, V., Trivić, S., Pericin, D., 2002. The three zinc-containing alcohol dehydrogenases from baker's yeast, Saccharomyces cerevisiae. FEMS Yeast Res. 2 (4), 481–494.
Li, D.D., Deng, L., Hu, G.H., Zhao, L.X., Hu, D.D., Jiang, Y.Y., Wang, Y., 2013. Using Galleria mellonella-*Candida albicans* infection model to evaluate antifungal agents. Biol. Pharm. Bull. 36 (9), 1482–1487.
Li, S.X., Song, Y.J., Zhang, Y.S., Wu, H.T., Guo, H., Zhu, K.J., Li, D.M., Zhang, H., 2017. Mitochondrial complex V α subunit is critical for *Candida albicans* pathogenicity through modulating multiple virulence factors. Front. Microbiol. 23 (8), 285.
Lo, H.J., Köhler, J.R., DiDomenico, B., Loebenberg, D., Cacciapuoti, A., Fink, G.R., 1997. Nonfilamentous *C. albicans* mutants are avirulent. Cell 90 (5), 939–949.
McClelland, E.E., Ramagopal, U.A., Rivera, J., Cox, J., Nakouzi, A., Prabu, M.M., Almo, S.C., Casadevall, A., 2016. A small protein associated with fungal energy metabolism affects the virulence of *Cryptococcus neoformans* in mammals. PLoS Pathog. 12 (9), e1005849.
Muhammed, M., Coleman, J.J., Mylonakis, E., 2012. *Caenorhabditis elegans*: a nematode infection model for pathogenic fungi. Methods Mol. Biol. 845, 447–454.
Mukherjee, P.K., Mohamed, S., Chandra, J., Kuhn, D., Liu, S., Antar, O.S., Munyon, R., Mitchell, A.P., Andes, D., Chance, M.R., Rouabhia, M., Ghannoum, M.A., 2006. Alcohol dehydrogenase restricts the ability of the pathogen *Candida albicans* to form a biofilm on catheter surfaces through an ethanol-based mechanism. Infect. Immun. 74 (7), 3804–3816.
Nett, J.E., Marchillo, K., Spiegel, C.A., Andes, D.R., 2010. Development and validation of an *in vivo Candida albicans* biofilm denture model. Infect. Immun. 78, 3650–3659.
Nobile, C.J., Andes, D.R., Nett, J.E., Smith, F.J., Yue, F., Phan, Q.T., Edwards, J.E., Filler, S.G., Mitchell, A.P., 2006. Critical role of Bcr1-dependent adhesins in *albicans biofilm* formation *in vitro* and *in vivo*. PLoS Pathog. 2, e63.
Noble, S.M., Johnson, A.D., 2007. Genetics of *Candida albicans*, a diploid human fungal pathogen. Annu. Rev. Genet. 41, 193–211.
Pitarch, A., Abian, J., Carrascal, M., Sánchez, M., Nombela, C., Gil, C., 2004. Proteomics-based identification of novel *Candida albicans* antigens for diagnosis of systemic candidiasis in patients with underlying hematological malignancies. Proteomics 4 (10), 3084–3106.
Pukkila-Worley, R., Peleg, A.Y., Tampakakis, E., Mylonakis, E., 2009. *Candida albicans* hyphal formation and virulence assessed using a *Caenorhabditis elegans* infection model. Eukaryot. Cell 8 (11), 1750–1758.
Peeters, E., Nelis, H.J., Coenye, T., 2008. Comparison of multiple methods for quantification of microbial biofilms grown in microtiter plates. J. Microbiol. Methods 72, 157–165.
Ramage, G., VandeWalle, K., López-Ribot, J.L., Wickes, B.L., 2002. The filamentation pathway controlled by the Efg1 regulator protein is required for normal biofilm formation and development in *Candida albicans*. FEMS Microbiol. Lett. 214, 95–100.
Reuss, O., Vik, A., Kolter, R., Morschhäuser, J., 2004. The *SAT1*-flipper, an optimized tool for gene disruption in *Candida albicans*. Gene 341, 119–127.
Rodrigues, A.G., Mardh, P.A., Pina-Vaz, C., Martinez-de-Oliveira, J., Fonseca, A.F., 1999. Germ tube formation changes surface hydrophobicity of *Candida* cells. Infect. Dis. Obstet. Gynecol. 7 (5), 222–226.
Sasse, C., Morschhäuser, J., 2012. Gene deletion in *Candida albicans* wild type strains using the *SAT1*-flipping strategy. Methods Mol. Biol. 845, 3–17.
Sekine, H., Shimada, T., Hayashi, C., Ishiguro, A., Tomita, F., Yokota, A., 2001. H^+-ATPase defect in *Corynebacteriumglutamicum* abolishes glutamic acid production with enhancement of glucose consumption rate. Appl. Microbiol. Biotechnol. 57 (4), 534–540.
Singleton, D.R., Masuoka, J., Hazen, K.C., 2001. Cloning and analysis of a *Candida albicans* gene that affects cell surface hydrophobicity. J. Bacteriol. 183 (12), 3582–3588.
Spellberg, B., Johnston, D., Phan, Q.T., Edwards, J.E.Jr., French, S.W., Ibrahim, A.S., Filler, S.G., 2003. Parenchymal organ, and not splenic, immunity correlates with host survival during disseminated candidiasis. Infect. Immun. 71, 5756–5764.
Spellberg, C.B., Ibrahim, A.S., Edwards Jr, J.E., Filler, S.G., 2005. Mice with disseminated candidiasis die of progressive sepsis. J. Infect. Dis. 192, 336–343.
She, X., Khamooshi, K., Gao, Y., Shen, Y., Lv, Y., Calderone, R., Fonzi, W., Liu, W., Li, D., 2015. Fungal specific subunits of the *Candida albicans* mitochondrial complex I drive diverse cell functions including cell wall synthesis. Cell. Microbiol. 17, 1350–1364.
Vander Heiden, M.G., Cantley, L.C., Thompson, C.B., 2009. Understanding the Warburg effect: the metabolic requirements of cell proliferation. Science 324, 1029–1033.
Tao, L., Zhang, Y., Fan, S., Nobile, C.J., Guan, G., Huang, G., 2017. Integration of the tricarboxylic acid (TCA) cycle with cAMP signaling and Sfl2 pathways in the regulation of CO_2 sensing and hyphal development in *Candida albicans*. PLoS Genet. 13, e1006949.
Thomson, J.M., Gaucher, E.A., Burgan, M.F., De Kee, D.W., Li, T., Aris, J.P., Benner, S.A., 2005. Resurrecting ancestral alcohol dehydrogenases from yeast. Nat. Genet. 37 (6), 630–635.
Zhang, P., Li, H., Cheng, J., Sun, A.Y., Wang, L., Mirchevska, G., Calderone, R., Li, D., 2018a. Respiratory stress in mitochondrial electron transport chain complex mutants of *Candida albicans* activates Snf1 kinase response. Fungal Genet. Biol. 111, 73–84.
Zhang, E., Cao, Y., Xia, Y., 2018b. Ethanol dehydrogenase I contributes to growth and sporulation under low oxygen condition via detoxification of acetaldehyde in Metarhizium acridum. Front. Microbiol. 9, 1932.
Zhang, X., Guo, H., Gao, L., Song, Y., Li, S., Zhang, H., 2012. Molecular mechanisms underlying the tetrandrine-mediated reversal of the fluconazole resistance of Candida albicans. Pharm. Biol. 51, 749–752.
Zhu, W., Filler, S.G., 2010. Interactions of *Candida albicans* with epithelial cells. Cell. Microbiol. 12, 273–282.